

Weighted total variation regularization for inverse problems with significant null spaces

Martin Burger*, Ole Løseth Elvetun† and Bjørn Fredrik Nielsen‡

Abstract

We consider inverse problems with large null spaces, which arise in important applications such as in inverse ECG and EEG procedures. Standard regularization methods typically produce solutions in or near the orthogonal complement of the forward operator's null space. This often leads to inadequate results, where internal sources are mistakenly interpreted as being near the data acquisition sites – e.g., near or at the body surface in connection with EEG and ECG recordings.

To mitigate this, we previously proposed weighting schemes for Tikhonov and sparsity regularization. Here, we extend this approach to total variation (TV) regularization, which is particularly suited for identifying spatially extended regions with approximately constant values. We introduce a weighted TV-regularization method, provide supporting analysis, and demonstrate its performance through numerical experiments. Unlike standard TV regularization, the weighted version successfully recovers the location and size of large, piecewise constant sources away from the boundary, though not their exact shape.

Additionally, we explore a hybrid weighted-sparsity and TV regularization approach, which better captures both small and large sources, albeit with somewhat more blurred reconstructions than the weighted TV method alone.

Keywords: Weighted total variation regularization, null space, ECG, EEG, hybrid weighted-sparsity and total variation.

1 Introduction

We will consider the problem

$$\min_{f \in BV(\Omega)} \left\{ \frac{1}{2} \|Kf - d\|_{L^2(E)}^2 + \alpha TV_w(f) \right\},$$

*Helmholtz Imaging, Deutsches Elektronen Synchrotron DESY, Notkestr. 85, 22607 Hamburg, Germany, and Department of Mathematics, University of Hamburg, Bundesstr. 55, 20146 Hamburg, Germany.

†Faculty of Science and Technology, Norwegian University of Life Sciences. Email: ole.elvetun@nmbu.no.

‡Faculty of Science and Technology, Norwegian University of Life Sciences. Email: bjorn.f.nielsen@nmbu.no.

where $K : L^2(\Omega) \rightarrow L^2(E)$ is a linear and non-injective compact operator, $\Omega \subset \mathbb{R}^n$, $n = 1, 2$, and E is the observation domain. The weighted regularization functional $TV_w : BV(\Omega) \rightarrow \mathbb{R}$ is defined by

$$\begin{aligned} TV_w(f) &= \int_{\Omega} |\omega(x) \nabla f(x)|_1 dx \\ &= \int_{\Omega} w_1(x) |\partial_{x_1} f(x)| + w_2(x) |\partial_{x_2} f(x)| dx, \end{aligned}$$

provided that $f \in W^{1,1}(\Omega)$. For any $f \in BV(\Omega) \setminus W^{1,1}(\Omega)$, the definition relies on the well-known dual formulation of the TV-functional presented in Section 3. Note that we employ the anisotropic version of TV and that we assume that $\omega(x)$ is a diagonal weight matrix with non-negative and measurable functions $w_1(x)$ and $w_2(x)$ at the diagonal. Their precise form is discussed below.

This work is motivated by the need, in many applications, to estimate the source term f in an equation in the form

$$Kf = d. \quad (1)$$

Assuming that f has a "blocky" structure, one would typically want to apply TV-regularization to this problem because this technique has proven to handle deblurring tasks very well, see, e.g., [4, 5].

For standard imagination problems, K equals the identity operator I , and one can employ the uniform weights $w_1(x) = w_2(x) = 1$, $x \in \Omega$, without introducing any further¹ bias. On the other hand, when K has a significant null space, the textbook form of TV-regularization might produce results of rather low quality: Figure 1 shows computations undertaken with $K = T(-\Delta + I)^{-1}$, where Δ represents the Laplace operator, I is the identity, $T : H^1(\Omega) \rightarrow L^2(\partial\Omega)$ is the trace operator and $\Omega = (0, 1) \times (0, 1)$. That is, we seek to use boundary data $d \in L^2(\partial\Omega)$ to recover the source term f in the following equations

$$\begin{aligned} -\Delta u + u &= f, \quad x \in \Omega, \\ \nabla u \cdot \mathbf{n} &= 0, \quad x \in \partial\Omega. \end{aligned}$$

We refer to pages 159–161 in [9] for a discussion of why standard regularization schemes fail to handle this type of problem adequately.

In this paper, we define the weight functions $w_1(x)$ and $w_2(x)$ in terms of the forward mapping and the (partial) derivatives of the Green's function of a suitable differential operator. This enables the recovery in 1D of single-jump-sources, i.e., shifted Heaviside functions, from boundary data, which is proven in Section 4. The ideas are extended to 2D problems in Section 5, including some theory. Section 7 contains a series of numerical experiments, which reveal that the weighted approach yields significantly better results than the standard TV scheme. In fact, the position and size of the source are estimated rather

¹TV-regularization yields a "blocky" biased, i.e., a preference for reconstructions with small total variation.

well, but its shape cannot be recovered, unless some rather strict conditions are satisfied.

Section 6 contains a discussion and analysis of a hybrid weighted-sparsity and TV regularization approach, which turns out to be better suited at identifying both small and larger sources. Moreover, its analysis is transparent, leading to short proofs of its approximate reconstruction capabilities. However, it yields somewhat more blurred recoveries than the (pure) weighted TV methodology.

The present text may be considered as a follow-up work to our earlier investigations of similar issues for Tikhonov and sparsity regularization [10, 13, 11, 12]. Nevertheless, it turns out that not only the implementation of the weighted versions of the former methods is easier than the numerical treatment of weighted TV, but also their analysis is more accessible. This is due to the fact that Tikhonov and sparsity regularization can be employed to identify small- and medium-sized local sources, whereas the TV approach typically is studied in terms of its capacity to detect borders between larger subregions.

There are many papers discussing and analyzing various weighting procedures in connection with total variation regularization, covering theory, numerics, and applications, e.g., [7, 14, 15, 16, 18, 19]. Nevertheless, as far as the authors know, this is the first text focusing on how to improve the performance of TV schemes when applied to inverse problems with significant null spaces.

2 Two versions of weighted TV-regularization

As mentioned above, our weights are defined in terms of the images under the forward operator K of the partial derivatives of suitable Green's functions. To be more concrete, let us consider the Green's functions for the Laplace operator, using homogeneous Dirichlet or Neumann boundary conditions:

$$\begin{aligned} -\Delta G^D &= \delta_x \quad \text{in } \Omega, & -\Delta G^N &= \delta_x - \frac{1}{|\Omega|} \quad \text{in } \Omega, \\ \underbrace{G^D = 0,}_{\text{Green's problem w/ Dirichlet B.C.}} \quad \text{on } \partial\Omega, & & \underbrace{\frac{\partial G^N}{\partial n} = 0}_{\text{Green's problem w/ Neumann B.C.}} & \quad \text{on } \partial\Omega. \end{aligned} \tag{2}$$

Here, $\delta_x(y) = \delta(y - x)$, where δ denotes the delta function/distribution.

As will become evident below, a crucial step in defining our TV-weights is to express the source term f in (1) in terms of ∇G^D or ∇G^N :

$$\begin{aligned} f(x) &= \int_{\Omega} f(y) \delta_x(y) dy \\ &= - \int_{\Omega} \Delta G^D(y; x) f(y) dy \\ &= \int_{\Omega} \nabla G^D(y; x) \cdot \nabla f(y) dy - \int_{\partial\Omega} f(y) \partial_n G^D(y; x) dS(y), \end{aligned} \tag{3}$$

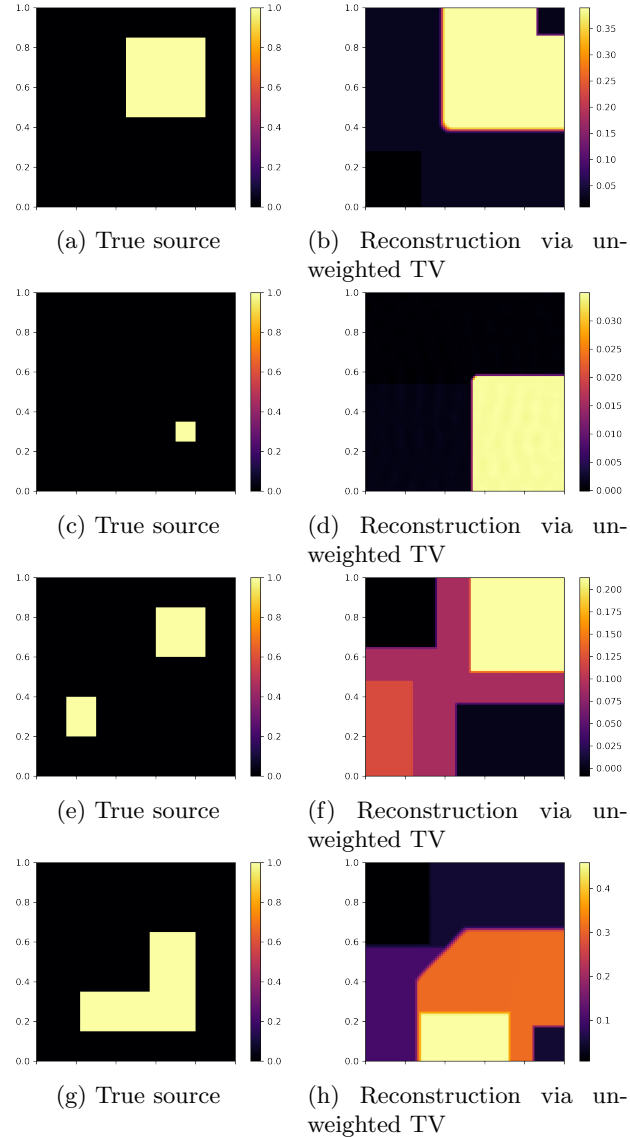


Figure 1: True sources and inverse recoveries computed with standard total variation regularization. No noise was added to the synthetic boundary data $d = Kf_{\text{true}}$ and $\alpha = 10^{-6}$.

or, similarly,

$$\begin{aligned}
f(x) &= \int_{\Omega} f(y) \delta_x(y) dy \\
&= - \int_{\Omega} \left(\Delta G^N(y; x) + \frac{1}{|\Omega|} \right) f(y) dy \\
&= \int_{\Omega} \nabla G^N(y; x) \cdot \nabla f(y) dy + \frac{1}{|\Omega|} \int_{\Omega} f(y) dy.
\end{aligned} \tag{4}$$

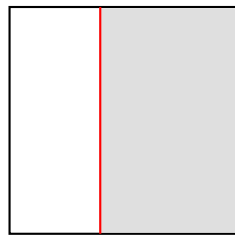
From (3) we find that

$$(Kf)(z) = K \left(\int_{\Omega} \nabla G^D(y; \cdot) \cdot \nabla f(y) dy - \int_{\partial\Omega} f(y) \partial_{\mathbf{n}} G^D(y; \cdot) dS(y) \right) (z), \tag{5}$$

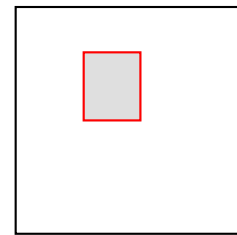
and similarly for (4). This expression for Kf motivates, at least to some extent, why suitable weights for TV-regularization might be defined in terms of the images of the partial derivatives of a Green's function: Note that (5) involves, potentially in a measure-theoretical sense, ∇f which is used in the standard definition of the total variation of f .

Whether f should be expressed in the form (3) or (4) in the derivation of the weights depends on the problem under consideration. To expand on this, consider Figure 2: If we are mainly searching for sources with a jump discontinuity stretching throughout the entire domain Ω (panel (a)), it turns out that it is beneficial to apply Neumann boundary conditions, as we do not wish to penalize the support of f along the boundary $\partial\Omega$. If, on the other hand, we are searching for a source inside Ω (panel (b)), it is wise to keep the boundary integral, i.e., to employ (3), in order to not make it erroneously "cheap" to position the source along $\partial\Omega$.

In sections 4 and 5 we will use (4) and (3), respectively.



(a) Source with a jump discontinuity stretching throughout the entire domain.



(b) Source inside the domain (away from $\partial\Omega$).

Figure 2: A domain Ω , with boundary $\partial\Omega$, and the support (in gray) of two prototypical sources.

3 Weighted total variation

In the following, we provide the basic definitions of weighted total variation to be used throughout.

3.1 Weighted total variation

Let us introduce the dual space notation

$$\mathcal{D} = \{\phi \in C_c^1(\Omega; \mathbb{R}^n) : |\phi_i(x)| \leq 1 \ \forall x \in \Omega, \ i \in \{1, \dots, n\}\},$$

and the weighted dual space

$$\mathcal{D}_w = \{\phi \in C_c^1(\Omega; \mathbb{R}^n) : |\phi_i(x)| \leq w_i(x) \ \forall x \in \Omega, \ i \in \{1, \dots, n\}\}. \quad (6)$$

We can then define the TV-norm

$$TV(f) = \sup_{\phi \in \mathcal{D}} \int_{\Omega} f(x) \operatorname{div} \phi(x) dx,$$

and similarly the weighted TV-norm

$$TV_w(f) = \sup_{\phi \in \mathcal{D}_w} \int_{\Omega} f(x) \operatorname{div} \phi(x) dx. \quad (7)$$

Invoking Riesz' representation theorem, we can define the bounded Radon measure Df on Ω , for any $f \in BV(\Omega)$, by

$$\int_{\Omega} f(x) \operatorname{div} \phi(x) dx = - \int_{\Omega} \phi(x) \cdot Df(x), \quad \forall \phi \in C_c^1(\Omega; \mathbb{R}^n). \quad (8)$$

It follows that the variation of this measure is precisely the total variation of the generating function $f \in BV(\Omega)$, i.e.,

$$\int_{\Omega} |Df(x)| = TV(f),$$

see, e.g., [20] for details. Similarly, the weighted version can be written in the form

$$TV_w(f) = \sum_{i=1}^n \int_{\Omega} w_i(x) |D_i f(x)|, \quad (9)$$

where $D_i f$ represent the i 'th component of the vector-valued Radon measure Df .

3.2 Weighted extended total variation

We will now introduce a relaxed weighted dual space notation, where we do no longer assume compact support of the test functions. That is, we let

$$\mathcal{D}_w^e = \{\phi \in C^1(\bar{\Omega}; \mathbb{R}^n) : |\phi_i(x)| \leq w_i(x) \ \forall x \in \bar{\Omega}, \ i \in \{1, \dots, n\}\}. \quad (10)$$

We can then define the extended weighted TV-functional

$$\overline{TV}_w(f) = \sup_{\phi \in \mathcal{D}_w^e} \int_{\Omega} f(x) \operatorname{div} \phi(x) dx. \quad (11)$$

Similarly to how we evaluated the TV-norm of f via its Radon measure Df on Ω , we now get the relation, cf. (3),

$$\overline{TV}_w(f) = \sum_{i=1}^n \int_{\Omega} w_i(x) |D_i f(x)| + \int_{\partial\Omega} w_{\partial}(x) |f(x)| dS(x), \quad (12)$$

where $w_{\partial} = \sum_i |n_i| w_i$ (n_i is the i 'th component of the outer unit normal vector of $\partial\Omega$).

4 1D analysis

In this section we focus on the one dimensional case, i.e., $\Omega = (0, 1)$. Let H_{x^*} denote the x^* -shifted Heaviside function

$$H_{x^*}(x) = H(x - x^*)$$

with associated shifted delta Dirac function δ_{x^*} . We will now analyze the following "jump pursuit" problem

$$\min_{f \in BV(0,1)} TV_w(f) \text{ subject to } Kf = K(\rho H_{x^*} + \tau), \quad (13)$$

where ρ and τ are constants incorporating the hight of the jump and the "base line" of the jump function, respectively, and $w(x)$ is an appropriate weight function (defined below).

We will prove that $\rho H_{x^*} + \tau$ solves (13). This is a challenging issue in the present context because the involved forward operator $K : L^2(0,1) \rightarrow L^2(E)$ has a nontrivial null space, i.e., E is typically a subset of $\bar{\Omega}$. Note that our analysis covers the boundary-observations-only case $E = \{0, 1\}$. Moreover, our exploration is not limited to state equations defined in terms of elliptic PDEs, but rather holds for general linear maps K with significant null spaces.

As will become clear below, functions with zero integral play an important role in this section:

$$\bar{f}(x) = f(x) - \int_0^1 f(z) dz,$$

and in particular

$$\bar{H}_y(x) = H_y(x) - \int_0^1 H_y(z) dz = \begin{cases} y-1, & x < y, \\ y, & x > y. \end{cases} \quad (14)$$

The total variation of functions which only differ by a constant is the same. Therefore, the image under K of the constant function 1 plays an important role in the present context. More precisely, defining the orthogonal projection onto the orthogonal complement of the space spanned by $K1$,

$$Q : L^2(E) \rightarrow \{tK1 \mid t \in \mathbb{R}\}^\perp, \quad (15)$$

we define the weight function to be used in connection with TV regularization in 1D as follows

$$w(y) = \|C\bar{H}_y\|_{L^2(E)}, \quad y \in \Omega, \quad (16)$$

where

$$C = QK. \quad (17)$$

Note that, $Cd = 0$ for any constant (function) d .

Remarks

Recall the definition (14) of $\bar{H}_y(x)$. Consider the function

$$G(y; x) = - \begin{cases} \frac{1}{2}y^2 + \frac{1}{2}x^2 - y, & x < y, \\ \frac{1}{2}y^2 + \frac{1}{2}x^2 - x, & x > y, \end{cases}$$

which satisfies

$$\frac{d}{dy}G(y; x) = -\bar{H}_y(x)$$

and

$$\frac{d^2}{dy^2}G(y; x) = \delta_x(y) - 1,$$

cf. (2), the version with homogeneous Neumann boundary conditions. This choice of a Green's function in the present situation is motivated by the fact that we want to recover a single-jump source $\rho H_{x^*} + \tau$, and this constitute the 1D version of the source depicted in panel (a) in Figure 2.

We emphasize that, in this section, the weighting is not defined in terms of the original forward operator K , but we rather use the modified operator C . Note that any solution f of (1) also satisfies $QKf = Qd$. The rationale behind this choice will become clear below.

4.1 Jump pursuit

We need two lemmas in order to prove the abovementioned recovery result for (13).

Lemma 4.1. *Assume that $f \in BV(0, 1)$ and let \bar{H}_y be defined as in (14). Then, recalling the definition (8) of the Radon measure Df , we can write*

$$f(x) = \int_0^1 \bar{H}_y(x) Df(y) + \eta \quad \text{a.e.}, \quad (18)$$

for η a constant.

(Before we prove this lemma, we observe the similarities between equations (18) and (4), keeping in mind that \bar{H}_y is the derivative of the aforementioned Green's function \bar{G}_y .)

Proof. We will derive the result by multiplying both sides of (18) by the derivative of an arbitrary smooth function ϕ with compact support and integrate, showing that these integrals become identical. That is, we will show that

$$\int_0^1 f(x) \phi'(x) dx = \int_0^1 \left(\int_0^1 \bar{H}_y(x) Df(y) \right) \phi'(x) dx \quad \forall \phi \in \mathcal{D}. \quad (19)$$

Indeed, by the definition of the Radon measure, the left-hand side satisfies

$$\int_0^1 f(x) \phi'(x) dx = - \int_0^1 \phi(x) Df(x). \quad (20)$$

A straightforward computation reveals that, for any $\phi \in \mathcal{D}$,

$$\begin{aligned} \int_0^1 \bar{H}_y(x) \phi'(x) dx &= \int_0^y (y-1) \phi'(x) dx + \int_y^1 y \phi'(x) dx \\ &= y [\phi(x)]_0^1 - [\phi(x)]_0^y \\ &= -\phi(y). \end{aligned} \quad (21)$$

Using Fubini's theorem, we get that the right-hand side of (19) obeys

$$\begin{aligned} \int_0^1 \left(\int_0^1 \bar{H}_y(x) Df(y) \right) \phi'(x) dx &= \int_0^1 \left(\int_0^1 \bar{H}_y(x) \phi'(x) dx \right) Df(y) \\ &= - \int_0^1 \phi(y) Df(y). \end{aligned} \quad (22)$$

Equality (19) now follows from (20) and (22).

Before proceeding, note that

$$\begin{aligned} \int_0^1 \left| \int_0^1 \bar{H}_y(x) Df(y) \right| dx &\leq \int_0^1 \int_0^1 |\bar{H}_y(x)| dx |Df(y)| \\ &\leq \int_0^1 |Df(y)| < \infty, \end{aligned} \quad (23)$$

which shows that $\int_0^1 \bar{H}_y(x) Df(y) \in L^1(0, 1)$.

Now, by rewriting (19) as

$$\int_0^1 \left[f(x) - \int_0^1 \bar{H}_y(x) Df(y) \right] \phi'(x) dx = 0 \quad \forall \phi \in \mathcal{D},$$

it only remains to show that this will imply that $g(x) := f(x) - \int_0^1 \bar{H}_y(x) Df(y)$ is constant a.e. Clearly, from (23) and since $f \in BV(0, 1)$, we conclude that $g \in L^1(0, 1)$. Furthermore, since the weak derivative of g equals zero, it immediately follows that $g \in W^{1,1}(0, 1)$. Therefore, from the fundamental lemma of calculus of variations, and a standard argument using mollifiers, we get that $g(x) = \eta$ a.e., which completes the proof. \square

Next, we argue that the proposed weight function is continuous, which implies that $TV_w(f)$ is well-defined for any $f \in BV(0, 1)$.

Lemma 4.2. *Let $w : \Omega \rightarrow \mathbb{R}_+$ be defined as in (16) and assume that $K : L^2(0, 1) \rightarrow L^2(E)$ is continuous. Then $w \in C(\Omega)$.*

Proof. It is a straightforward calculation to show that the map $y \mapsto \bar{H}_y$ is continuous as a mapping from $\Omega = (0, 1)$ to $L^p(0, 1)$, $1 \leq p < \infty$. Since we assume that K is continuous and the orthogonal projection Q is continuous, it follows that $C = QK$ and consequently $y \mapsto \|C\bar{H}_y\|_{L^2(E)}$ are continuous. \square

Theorem 4.3. *Let w be the weight function defined in (16). Then, $\rho H_{x^*} + \tau$ solves the jump pursuit problem (13).*

Proof. We could use the Lebesgue decomposition of \bar{H}_{x^*} to show that the measure $D\bar{H}_{x^*}$ becomes the Dirac mass δ_{x^*} . Alternatively, we can obtain this result from the distributional definition, employing (7), (21) and (6),

$$\begin{aligned} TV_w(\rho \bar{H}_{x^*}) &= \sup_{\phi \in \mathcal{D}_w} \int_0^1 \rho \bar{H}_{x^*}(x) \phi'(x) dx = \sup_{\phi \in \mathcal{D}_w} \{-\rho \phi(x^*)\} \\ &= |\rho| w(x^*). \end{aligned} \tag{24}$$

Finally, we can now show the main result. Consider any $f \in BV(0, 1)$ for which $Kf = K(\rho H_{x^*} + \tau)$, or $Cf = C(\rho H_{x^*})$ because C annihilates constants, cf. (17). We get, recalling (24) and the definition (16) of the weight function w ,

$$\begin{aligned} TV_w(\rho \bar{H}_{x^*} + \tau) &= TV_w(\rho \bar{H}_{x^*}) = |\rho| w(x^*) = |\rho| \|CH_{x^*}\|_{L^2(E)} \\ &= \|C(\rho H_{x^*})\|_{L^2(E)} = \|C(\rho H_{x^*} + \tau)\|_{L^2(E)} = \|Cf\|_{L^2(E)} \\ &= \left(\int_E \left[\left(\int_0^1 C\bar{H}_y(\cdot) Df(y) \right) \right]^2 dz \right)^{1/2} \\ &\leq \int_0^1 \left(\int_E [C\bar{H}_y(\cdot)]^2 dz \right)^{1/2} |Df(y)| = \int_0^1 w(y) |Df(y)| \\ &= TV_w(f), \end{aligned}$$

where we have used Lemma 4.1 in the seventh equality. We have also employed Minkowski's integral inequality and that

$$C \left(\int_0^1 \bar{H}_y(\cdot) Df(y) + \eta \right) = \int_0^1 C \bar{H}_y(\cdot) Df(y),$$

which holds because the mapping $g : (0, 1) \rightarrow BV(0, 1)$, $y \mapsto \bar{H}_y(\cdot)$ is Bochner integrable and $C\eta = 0$. \square

Remark

Here, we defined the weight function $w(y)$ in terms of the L^2 -norm, see (16). Since Minkowski's integral inequality holds for L^p -norms, Theorem 4.3 also holds if one employs the weight function

$$w(y) = \|C\bar{H}_y\|_{L^p(E)}, \quad y \in \Omega,$$

and $1 \leq p < \infty$, provided that $Cd = 0$ for any constant d , jmf. (17). The latter would require that one can define an appropriate operator Q .

4.2 Regularized problem

Let us also consider the associated variational formulation

$$\min_{f \in BV(0,1)} \left\{ \frac{1}{2} \|Kf - K(\rho\bar{H}_{x^*} + \tau)\|^2 + \alpha TV_w(f) \right\}. \quad (25)$$

The proof of the following theorem is presented in Appendix A.

Theorem 4.4. *Let w be the weight function defined in (16). Then,*

$$f_\alpha = \gamma\rho\bar{H}_{x^*} + \eta$$

solves the weighted total variational regularization problem (25), where

$$\gamma = 1 - \frac{\alpha}{|\rho|\|C\bar{H}_{x^*}\|} \quad \text{and} \quad \eta = \tau + \frac{(1-\gamma)\rho(K\bar{H}_{x^*}, K1)}{\|K1\|^2},$$

provided that $0 < \alpha < |\rho|\|C\bar{H}_{x^}\|$. Note that $\gamma \rightarrow 1$ and $\eta \rightarrow \tau$ as $\alpha \rightarrow 0$.*

Let us also mention that the analysis above can also be carried out in the abstract framework of singular vectors and ground states as defined in [3] (see also [8] for a more recent overview). While we give explicit computations in this paper for the sake of self-containedness it is worth noting that for the original total variation the step function with jump in the mid point is the ground state (corresponding to the lowest singular value), while jumps moving to the boundary result in increasing singular values and thus increasing bias (respectively reconstruction error). With the above the definition of the weighted total variation the singular values with respect to this new seminorm are equilibrated.

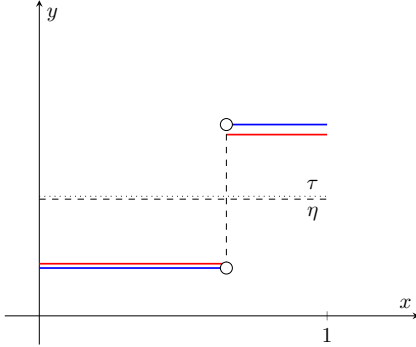


Figure 3: A visualization of how the exact solution $\rho \bar{H}_{x^*} + \tau$ (in blue color) and the inverse solution f_α (in red color) presented in Theorem 4.4 are related. The jump is correctly located, but slightly smaller and the center line is slightly shifted depending on the inner-product $(K \bar{H}_{x^*}, K1)$.

5 2D analysis

In 1D we defined the weights in terms of the shifted Heaviside function (14). And, as made clear by the proofs of theorems 4.3 and 4.4, the crucial step in showing that (13) and (25) admit "one-jump" minimizers lies in the relationship between the Heaviside function \bar{H}_{x^*} and the Dirac mass δ_{x^*} . The purpose of this section is to generalize these ideas to 2D. To that end, it is useful to recall that one may regard \bar{H}_{x^*} as a derivative of a Green's function associated with x^* .

Given $\Omega \subset \mathbb{R}^2$, let $G(x; x^*)$ be a Green's function associated with this domain with a singularity at x^* and subject to homogeneous Dirichlet boundary conditions, cf. (3) and the discussion in Section 2. Keeping the close connection between the Dirac function δ_{x^*} and $G(x; x^*)$ in mind, we can express a function $f : \Omega \rightarrow \mathbb{R}$ in the form

$$\begin{aligned}
 f(x) &= \int_{\Omega} f(y) \delta_x(y) dy = - \int_{\Omega} f(y) \Delta_y G(y; x) dy \\
 &= \int_{\Omega} \nabla_y G(y; x) \cdot Df(y) - \int_{\partial\Omega} f(y) \partial_n G(y; x) dS(y) \\
 &= \int_{\Omega} \nabla_y G(x; y) \cdot Df(y) - \int_{\partial\Omega} f(y) \partial_n G(x; y) dS(y),
 \end{aligned}$$

where we used the symmetry of the Green's function in the last equality.

Now, assuming sufficient regularity, and following the 1D analysis, we get

the upper bound

$$\begin{aligned}
\|Kf\|_{L^1(E)} &= \int_E |(Kf)(z)| dz \\
&= \int_E \left| K \left[\int_{\Omega} \nabla f(y) \cdot \nabla_y G(\cdot; y) dy - \int_{\partial\Omega} f(y) \partial_{\mathbf{n}} G(\cdot; y) dS(y) \right] \right| dz \\
&= \int_E \left| \int_{\Omega} \partial_{y_1} f(y) K \partial_{y_1} G(\cdot; y) dy + \int_{\Omega} \partial_{y_2} f(y) K \partial_{y_2} G(\cdot; y) dy \right. \\
&\quad \left. - \int_{\partial\Omega} f(y) K \partial_{\mathbf{n}} G(\cdot; y) dS(y) \right| dz \\
&\leq \int_{\Omega} \left[\int_E |K \partial_{y_1} G(\cdot; y)| dz \right] |\partial_{y_1} f(y)| dy \\
&\quad + \int_{\Omega} \left[\int_E |K \partial_{y_2} G(\cdot; y)| dz \right] |\partial_{y_2} f(y)| dy \\
&\quad + \int_{\partial\Omega} \left[\int_E |K \partial_{\mathbf{n}} G(\cdot; y)| dz \right] |f(y)| dS(y) := \overline{TV}_w(f), \tag{26}
\end{aligned}$$

where the weights are defined by

$$\begin{aligned}
w_1(y) &= \int_E |K \partial_{y_1} G(\cdot; y)| dz, \\
w_2(y) &= \int_E |K \partial_{y_2} G(\cdot; y)| dz, \\
w_{\partial}(y) &= \int_E |K \partial_{\mathbf{n}} G(\cdot; y)| dz.
\end{aligned}$$

Note that w_{∂} is only present when the Green's function is generated using Dirichlet boundary conditions. Here we use Dirichlet boundary conditions because we want to recover sources well/properly inside Ω , cf. Section 2.

Remark 5.1. Note that in (26) we could have used any L^p -norm and employed Minkowski's integral inequality to obtain

$$\begin{aligned}
\|Kf\|_{L^p(E)} &\leq \int_{\Omega} \|K \partial_{y_1} G(\cdot; y)\|_{L^p(E)} |\partial_{y_1} f(y)| dy \\
&\quad + \int_{\Omega} \|K \partial_{y_2} G(\cdot; y)\|_{L^p(E)} |\partial_{y_2} f(y)| dy \\
&\quad + \int_{\partial\Omega} \|K \partial_{\mathbf{n}} G(\cdot; y)\|_{L^p(E)} |f(y)| dS(y). \tag{27}
\end{aligned}$$

That is, provided sufficient regularity, we have the freedom to choose the L^p -norm for the weights, including $p = \infty$. Of course, this leads to different weights: $w_1(y) = \|K \partial_{y_1} G(\cdot; y)\|_{L^p(E)}$, etc.

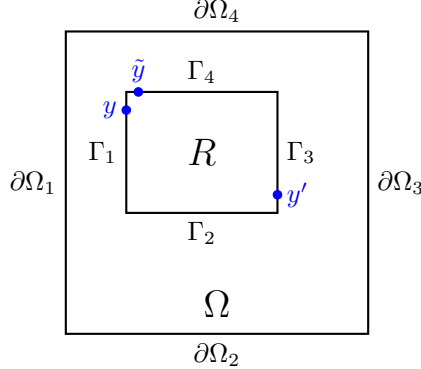


Figure 4: A rectangular domain Ω and the support $R \subset \Omega$, with boundary $\Gamma_1 \cup \Gamma_2 \cup \Gamma_3 \cup \Gamma_4$, of the true source $f^* = \chi_R$. The blue dots represent some arbitrary $y \in \Gamma_1$ and $y' \in \Gamma_3$.

Consider the problem

$$\min_{f \in BV(\Omega)} \overline{TV}_w(f) \quad \text{subject to} \quad Kf = Kf^*. \quad (28)$$

If the true source f^* obeys

$$\overline{TV}_w(f^*) = \|Kf^*\|_{L^1(E)}, \quad (29)$$

and f is any function satisfying

$$Kf = Kf^*,$$

then we can employ (26) to conclude that

$$\begin{aligned} TV_w(f^*) &= \|Kf^*\|_{L^1(E)} \\ &= \|Kf\|_{L^1(E)} \\ &\leq \overline{TV}_w(f). \end{aligned}$$

Consequently, f^* is a solution of (28).

Provided that suitable assumptions are fulfilled, we will now argue that (29) holds when $f^* = \chi_R$, where χ_R denotes the characteristic function of a rectangle, see Figure 4. Roughly speaking, our analysis requires disjoint images, under K , of the line integrals along $\Gamma_1, \Gamma_2, \Gamma_3, \Gamma_4$ of the normal derivatives of the Green's function. The second assumption (31), expresses that, for any fixed z , the sign of $K(\nabla_y G(\cdot; y) \cdot \mathbf{n}(y))(z)$ must be the same for all $y \in \Gamma_j$. These assumptions are discussed in somewhat more detail after the proof of the following result:

Theorem 5.2. *Assume that $f^* = \chi_R$, where $R = (a, b) \times (c, d) \subset \Omega$, cf. Figure 4. Also, we assume that the observation domain E can be decomposed into mutually disjoint sets E_j , $\cup_{j=1}^4 E_j = E$, for which the "sources" $\partial_{y_i} G(y; x)$ associated with the boundaries Γ_1 (left), Γ_2 (bottom), Γ_3 (right), and Γ_4 (top) of R obey the following:*

- For $j \in \{1, 2, 3, 4\}$:

$$\text{supp} \left(K \int_{\Gamma_j} \nabla_y G(\cdot; y) \cdot \mathbf{n}(y) d\sigma(y) \right) \subset E_j. \quad (30)$$

- For $j \in \{1, 2, 3, 4\}$: For each $z \in E_j$,

$$\text{sgn}[K(\nabla_y G(\cdot; y) \cdot \mathbf{n}(y))(z)] = c_j \quad \forall y \in \Gamma_j, \quad (31)$$

where $c_j \in \{-1, 0, 1\}$ is a constant.

Then,

$$f^* \in \arg \min_{f \in BV(\Omega)} \overline{TV}_w(f) \quad \text{subject to} \quad Kf = K\chi_R.$$

Proof. First, since $f^* = \chi_R$, we note that

$$\begin{aligned} TV(f^*) &= \int_{\Omega} w_1 |\partial_{x_1} f^*| + \int_{\Omega} w_2 |\partial_{x_2} f^*| + \int_{\partial\Omega} w_n |f^*| \\ &= \int_{\Gamma_1} w_1 + \int_{\Gamma_2} w_2 + \int_{\Gamma_3} w_1 + \int_{\Gamma_4} w_2. \end{aligned}$$

Secondly, we can express $f^* = \chi_R$ in the following form

$$\begin{aligned} \chi_R(x) &= \int_{\Omega} \chi_R(y) \delta_x(y) dy = - \int_{\Omega} \chi_R(y) \Delta G(y; x) dy = - \int_R \Delta G(y; x) dy \\ &= - \int_{\partial R} \nabla_y G(y; x) \cdot \mathbf{n}(y) d\sigma(y), = - \int_{\partial R} \nabla_y G(x; y) \cdot \mathbf{n}(y) d\sigma(y). \end{aligned}$$

Thus, if we evaluate Kf^* at a point $z \in E$ using the above representation of f^* , we get

$$\begin{aligned} (Kf^*)(z) &= - \left(K \int_{\partial R} \nabla_y G(\cdot; y) \cdot \mathbf{n}(y) d\sigma(y) \right) (z) \\ &= - \left(K \sum_i \int_{\Gamma_i} \nabla_y G(\cdot; y) \cdot \mathbf{n}(y) d\sigma(y) \right) (z). \end{aligned}$$

Consequently, we obtain, using (30) and (31) in the second and fifth equality

below, respectively,

$$\begin{aligned}
\|Kf^*\|_{L^1(E)} &= \int_E \left| \sum_i K \int_{\Gamma_i} (\nabla_y G(\cdot; y) \cdot \mathbf{n}(y)) d\sigma(y) \right| dz \\
&= \int_E \sum_i \left| \int_{\Gamma_i} K(\nabla_y G(\cdot; y) \cdot \mathbf{n}(y)) d\sigma(y) \right| dz \\
&= \sum_j \int_{E_j} \sum_i \left| \int_{\Gamma_i} K(\nabla_y G(\cdot; y) \cdot \mathbf{n}(y)) d\sigma(y) \right| dz \\
&= \int_{E_1} \left| - \int_{\Gamma_1} K \partial_{y_1} G(\cdot; y) d\sigma(y) \right| dz + \int_{E_2} \left| - \int_{\Gamma_2} K \partial_{y_2} G(\cdot; y) d\sigma(y) \right| dz \\
&\quad + \int_{E_3} \left| \int_{\Gamma_3} K \partial_{y_1} G(\cdot; y) d\sigma(y) \right| dz + \int_{E_4} \left| \int_{\Gamma_4} K \partial_{y_2} G(\cdot; y) d\sigma(y) \right| dz \\
&= \int_{\Gamma_1} \int_{E_1} |K \partial_{y_1} G(\cdot; y)| dz d\sigma(y) + \int_{\Gamma_2} \int_{E_2} |K \partial_{y_2} G(\cdot; y)| dz d\sigma(y) \\
&\quad + \int_{\Gamma_3} \int_{E_3} |K \partial_{y_1} G(\cdot; y)| dz d\sigma(y) + \int_{\Gamma_4} \int_{E_4} |K \partial_{y_2} G(\cdot; y)| dz d\sigma(y) \\
&= \int_{\Gamma_1} w_1 + \int_{\Gamma_2} w_2 + \int_{\Gamma_3} w_1 + \int_{\Gamma_4} w_2 = \overline{TV}_w(f^*).
\end{aligned}$$

The result now follows from (26). \square

Note that Theorem 5.2 holds whenever Ω , R and K are such that (30) and (31) hold for a finite number of sets $\{E_j\}$ and $\{\Gamma_j\}$. That is, the argument is not restricted to the rectangle-inside-rectangle setup, which we decided to consider for an easy exposition. Nevertheless, f^* must be the characteristic function of the subdomain R .

We will now motivate why assumptions (30) and (31) are (approximately) satisfied when K exhibits a strong diffusive effect, provided that we consider a rectangle-inside-rectangle scenario; see Figure 4. To this end, consider the specific case where $E = \partial\Omega$, that is, $K : BV(\Omega) \rightarrow L^1(\partial\Omega)$.

In this setting, let us examine the two Green functions that have singularities at the points y and y' , respectively; cf. Figure 4. The normal derivatives of these Green's functions resemble horizontally oriented dipoles. Due to the strong diffusive property of K , the image of $\partial_{y_1} G(\cdot, y)$, $y \in \Gamma_1$, under K has most of its relative magnitude concentrated along $\partial\Omega_1$, while the image of $\partial_{y_2} G(\cdot, y')$, $y \in \Gamma_3$, under K is relatively concentrated along $\partial\Omega_3$. A similar property hold for Green's functions associated with points located along Γ_2 and Γ_4 .

When comparing sources located along vertical and horizontal line segments — for example $y \in \Gamma_1$ and $\tilde{y} \in \Gamma_4$, we consider the images of $\partial_{y_1} G(\cdot, y)$ and $\partial_{y_2} G(\cdot, \tilde{y})$ under K . These correspond to images of horizontally and vertically oriented dipole structures, which implies that these images are (relatively) concentrated on $\partial\Omega_1$ and $\partial\Omega_4$, respectively.

Based on the discussion presented in the last two paragraphs, we conclude that (roughly) (30) and (31) are satisfied with $E_j = \partial\Omega_j$, $j = 1, 2, 3, 4$. We

also remark that when the rectangle is small or thin, then $y \in \Gamma_1$ and $y' \in \Gamma_3$ are close to each other, making the assumption of disjoint images under K of the partial derivatives of the involved Green's function more dubious. In the numerical experiments section, we will see this effect quite clearly: small rectangles are overestimated (in size) in the recovery process.

6 Hybrid regularization method

We will see in the numerical experiments section that weighted TV-regularization has a tendency to overestimate the size of small sources. This suggests that it might be beneficial to combine weighted TV-regularization with sparsity regularization, incorporated in terms of a measure theoretical framework in the infinite dimensional setting:

$$\min_{f \in BV(\Omega)} \left\{ \frac{1}{2} \|K\mu - d\|_{L^2(E)}^2 + \alpha TV_w(f) + \beta \|\mu\|_{\mathcal{M}_{\tilde{w}}(\Omega)} \right\}, \quad (32)$$

where μ is the measure associated with f , see (38) below. In this section we thus assume that K operates on measures instead of functions, which is common when one considers sparsity regularization in an infinite dimensional setting. We now define the additional notation and the weight function \tilde{w} to be employed in the sparsity term.

Let $\mathcal{M}(\Omega)$ be the space of Radon measures and assume that we have a bounded linear operator $K : \mathcal{M}(\Omega) \rightarrow L^2(E)$ which admits the kernel representation

$$K\mu = \int_{\Omega} k(x, \cdot) d\mu(x),$$

where $k : \Omega \times E \rightarrow \mathbb{R}$ and, as above, E denotes the observation domain. We define the weight function $\tilde{w} : \Omega \rightarrow \mathbb{R}$ by

$$\tilde{w}(x) = \|K\delta_x\|_{L^2(E)}, \quad (33)$$

where δ_x is the Dirac measure associated with the point $x \in \Omega$ and we assume that there exist constants \tilde{w}_{\min} and \tilde{w}_{\max} such that

$$0 < \tilde{w}_{\min} \leq \tilde{w}(x) \leq \tilde{w}_{\max} < \infty, \quad \forall x \in \Omega.$$

This also enables us to introduce the weighted Radon space $\mathcal{M}_{\tilde{w}}(\Omega)$ equipped with the norm²

$$\|\mu\|_{\mathcal{M}_{\tilde{w}}(\Omega)} = \int_{\Omega} \tilde{w}(x) d|\mu|,$$

where $|\mu|$ is the total variation measure of μ .

²The map $x \mapsto \int_E |k(x, y)|^2 d\nu(y)$ is measurable (as a pointwise integral over measurable functions), and therefore the map $x \mapsto \|K\delta_x\|_{L^2(E)}$ is measurable, which justifies the weighted norm.

Let $R \subset \Omega$ be a set of finite perimeter. Since $\chi_R \in L^1_{loc}(\Omega)$, it follows that

$$\mu_R(A) = \int_A \chi_R(x) dx, \quad (34)$$

where $A \subset \Omega$ is any Lebesgue measurable set, defines a Radon measure μ_R . Let μ_R constitute the true source, for which we use the notation;

$$\mu^* = \mu_R, \quad (35)$$

which consistent with the symbolism used in the previous sections. Also, assume that the following relation between the subdomain R and the forward operator holds: There exist a continuous function $\tau : \Omega \rightarrow \mathbb{R}$ and a point $\bar{x} \in R$ such that

$$K\delta_z = \tau(z)K\delta_{\bar{x}}, \quad \tau(z) > 0, \quad \forall z \in R. \quad (36)$$

That is, we assume that the images under K of the individual Dirac measures associated with the points in R are parallel. (Typically, $\tau(z) \approx 1$, reflecting the smoothing property of the forward mapping). Roughly speaking, it is plausible that (36) approximately holds provided that the extent of the region R is not too large compared with R 's distance to the boundary $\partial\Omega$, provided that $E = \partial\Omega$. Under these circumstances, we will now prove that the region R can be recovered, in a measure theoretical sense, by solving a sparsity basis pursuit problem. Thereafter, we employ this result to analyze the basis pursuit counterpart to (32) when $\alpha \rightarrow 0$ for a fixed $\beta > 0$

Proposition 6.1. *Let $\mu^* = \mu_R$ and assume that (36) holds. Then*

$$\mu^* \in \arg \min_{\mu \in \mathcal{M}(\Omega)} \|\mu\|_{\mathcal{M}_{\tilde{w}}(\Omega)} \quad \text{subject to} \quad K\mu = K\mu^*, \quad (37)$$

where $\tilde{w} : \Omega \rightarrow \mathbb{R}$ is defined in (33).

Proof. We first observe that the true source $\mu^* = \mu_R$ satisfies

$$\begin{aligned} \|\mu^*\|_{\mathcal{M}_{\tilde{w}}(\Omega)} &= \int_{\Omega} \tilde{w}(x) d\mu_R(x) = \int_R \tilde{w}(x) dx \\ &= \int_R \|K\delta_x\|_{L^2(E)} dx \\ &= \int_R \tau(x) dx \|K\delta_{\bar{x}}\|_{L^2(E)}, \end{aligned}$$

where we used (36) for the last line, and

$$\begin{aligned}
\|K\mu^*\|_{L^2(E)} &= \left\| \int_{\Omega} k(x, \cdot) d\mu_R(x) \right\|_{L^2(E)} = \left\| \int_R k(x, \cdot) dx \right\|_{L^2(E)} \\
&= \left\| \int_R \int_{\Omega} k(z, \cdot) d\delta_x(z) dx \right\|_{L^2(E)} \\
&= \left\| \int_R K\delta_x dx \right\|_{L^2(E)} \\
&= \left\| \int_R \tau(x) dx \ K\delta_{\bar{x}} \right\|_{L^2(E)} \\
&= \int_R \tau(x) dx \ \|K\delta_{\bar{x}}\|_{L^2(E)}.
\end{aligned}$$

Therefore, for any $\mu \in \mathcal{M}(\Omega)$ satisfying $K\mu = K\mu^*$,

$$\begin{aligned}
\|\mu^*\|_{\mathcal{M}_{\bar{w}}(\Omega)} &= \|K\mu^*\|_{L^2(E)} = \|K\mu\|_{L^2(E)} \\
&= \left\| \int_{\Omega} k(x, \cdot) d\mu(x) \right\|_{L^2(E)} \\
&\leq \int_{\Omega} \|K\delta_x\|_{L^2(E)} |d\mu(x)| \\
&= \int_{\Omega} \bar{w}(x) |d\mu(x)| \\
&= \|\mu\|_{\mathcal{M}_{\bar{w}}(\Omega)},
\end{aligned}$$

where we have used the relation $K\delta_x = k(x, \cdot)$ and also Minkowski's integral inequality. This completes the proof. \square

Remark 6.2. *If (36) holds, then it follows in a straightforward manner that $\hat{\mu} = \int_R \tau(x) dx \delta_{\bar{x}}$ also solves the minimization problem (37), i.e., $K(\hat{\mu}) = K\mu^*$ and $\|\hat{\mu}\|_{\mathcal{M}_{\bar{w}}(\Omega)} = \|\mu^*\|_{\mathcal{M}_{\bar{w}}(\Omega)}$. Hence, if one wants to identify a "blocky" structure while preventing underestimation of the size of small sources, it might be beneficial to combine sparsity methodologies with TV-regularization, which we now investigate further.*

It is well known that any $f \in BV(\Omega) \subset L^1(\Omega)$ introduces a measure by

$$\mu(A) = \int_A f(x) dx, \quad (38)$$

where $A \subset \Omega$ is any Lebesgue measurable set, cf. (34) that expresses this connection between the true measure $\mu^* = \mu_R$ and $f^* = \chi_R$. (f and f^* are in this context Radon–Nikodym derivatives.) In the sequel, we will use the set

$$\mathcal{U} = \left\{ \mu \in \mathcal{M}(\Omega) \mid f = \frac{d\mu}{dx} \in BV(\Omega) \right\},$$

and, when suitable, write $f\mathcal{L}^n$ for μ , i.e.,

$$f\mathcal{L}^n = \mu.$$

We also note that, in the following two propositions, we rely on the notation to distinguish between a measure μ_α (or the optimal μ^*) and the associated BV-function f_α (or the optimal f^*).

Let us verify that including weighted TV-regularization reduces the weighted TV-semi-norm of the solution:

Lemma 6.3. *Assume that $\mu^* = \mu_R$, that (36) holds and let*

$$\mu_\alpha \in \arg \min_{\mu \in \mathcal{U}} \{ \alpha TV_w(f) + \|\mu\|_{\mathcal{M}_{\tilde{w}}(\Omega)} \} \quad \text{subject to} \quad K\mu = K\mu^*, \quad (39)$$

where f is the BV-function associated with μ . Then, for $\alpha \geq 0$,

$$TV_w(f_\alpha) \leq TV_w(f^*)$$

and

$$0 \leq \|\mu_\alpha\|_{\mathcal{M}_{\tilde{w}}(\Omega)} - \|\mu^*\|_{\mathcal{M}_{\tilde{w}}(\Omega)} \leq \alpha TV_w(f^*).$$

Here, f_α and f^* denote the Radon–Nikodym derivatives of μ_α and μ^* , respectively.

Proof. It follows from (37) and (39) that

$$\alpha TV_w(f_\alpha) + \|\mu^*\|_{\mathcal{M}_{\tilde{w}}(\Omega)} \leq \alpha TV_w(f_\alpha) + \|\mu_\alpha\|_{\mathcal{M}_{\tilde{w}}(\Omega)} \leq \alpha TV_w(f^*) + \|\mu^*\|_{\mathcal{M}_{\tilde{w}}(\Omega)},$$

which implies that

$$TV_w(f_\alpha) \leq TV_w(f^*)$$

and that

$$0 \leq \|\mu_\alpha\|_{\mathcal{M}_{\tilde{w}}(\Omega)} - \|\mu^*\|_{\mathcal{M}_{\tilde{w}}(\Omega)} \leq \alpha TV_w(f^*) - \alpha TV_w(f_\alpha),$$

which completes the proof. \square

We next explain that, if (37) has several solutions, one might want to add weighted TV-regularization in order to choose/compute a "blocky" solution.

Proposition 6.4. *Let μ_α , with Radon–Nikodym derivative f_α , be as defined in (39). Suppose the true source μ^* satisfies (35) and (36), and that its associated Radon–Nikodym derivative f^* is the unique solution to the optimization problem*

$$f^* = \arg \min_{f \in S} TV_w(f), \quad (40)$$

where

$$S = \arg \min_{f \in BV(\Omega)} \|f\mathcal{L}^n\|_{\mathcal{M}_{\tilde{w}}(\Omega)} \quad \text{subject to} \quad Kf\mathcal{L}^n = Kf^*\mathcal{L}^n.$$

Then

$$\lim_{\alpha \rightarrow 0} f_\alpha = f^*, \quad \text{in } L^1(\Omega).$$

Proof. It follows from (39) that

$$\|f_\alpha\|_{BV(\Omega)} = \|f_\alpha\|_{L^1(\Omega)} + TV_w(f_\alpha) \leq \frac{1}{\tilde{w}_{\min}} \|\mu^*\|_{\mathcal{M}_{\tilde{w}}(\Omega)} + TV_w(f^*),$$

which implies that $\{f_\alpha\}_{\alpha>0} \subset BV(\Omega)$ is uniformly bounded. Consequently, Rellich's compactness theorem implies that we can extract a sequence (f_{α_k}) , $\alpha_k \rightarrow 0$, such that

$$f_{\alpha_k} \rightarrow \bar{f} \quad \text{in } L^1(\Omega),$$

for some $\bar{f} \in BV(\Omega)$ with associated measure $\bar{\mu} = \bar{f}\mathcal{L}^n$.

It follows from (39) that $K\mu_\alpha = K\mu^*$ and hence $K\mu_{\alpha_k} = K\mu^*$ for all k . Furthermore, due to the continuity of the forward operator $K : \mathcal{M}(\Omega) \rightarrow L^p(E)$, we find that

$$K\bar{f}\mathcal{L}^n = \lim_{k \rightarrow \infty} Kf_{\alpha_k}\mathcal{L}^n = \lim_{k \rightarrow \infty} K\mu_{\alpha_k} = K\mu^* = Kf^*\mathcal{L}^n. \quad (41)$$

Next, Lemma 6.3 yields that

$$0 \leq \|\mu_{\alpha_k}\|_{\mathcal{M}_{\tilde{w}}(\Omega)} - \|\mu^*\|_{\mathcal{M}_{\tilde{w}}(\Omega)} \leq \alpha_k TV_w(f^*)$$

or

$$0 \leq \|f_{\alpha_k}\mathcal{L}^n\|_{\mathcal{M}_{\tilde{w}}(\Omega)} - \|f^*\mathcal{L}^n\|_{\mathcal{M}_{\tilde{w}}(\Omega)} \leq \alpha_k TV_w(f^*),$$

i.e., since $\alpha_k \rightarrow 0$,

$$\|\bar{f}\mathcal{L}^n\|_{\mathcal{M}_{\tilde{w}}} = \|f^*\mathcal{L}^n\|_{\mathcal{M}_{\tilde{w}}},$$

which combined with (41) show that \bar{f} is a feasible solution of (40).

To show that \bar{f} is optimal, we combine Lemma 6.3 with the fact that the total variation functional is lower semi-continuous with respect to L^1 to obtain the inequalities

$$TV_w(f^*) \geq \liminf_k TV_w(f_{\alpha_k}) \geq TV_w(\bar{f}).$$

It follows that \bar{f} is a solution of (40), and we can conclude that $\bar{f} = f^*$ because f^* is assumed to be the unique minimizer of (40).

This argument also shows that *any* convergent sequence $(f_{\alpha_k}) \subset \{f_\alpha\}_{\alpha>0}$, $\alpha_k \rightarrow 0$, must converge to f^* in $L^1(\Omega)$, which, due to the fact that $\{f_\alpha\}_{\alpha>0}$ is relative compact in $L^1(\Omega)$, will imply that $f_\alpha \rightarrow f^*$, as $\alpha \rightarrow 0$, in $L^1(\Omega)$. \square

Remark 6.5. *We remark that Lemma 6.3 and Proposition 6.4 also are valid if one replaces TV_w with standard total variation, denoted TV_I below. The proofs are identical, replacing TV_w with TV_I .*

7 Numerical experiments

We will perform numerical experiments on the unit square $\Omega = (0, 1) \times (0, 1)$ with the forward operator $K : L^2(\Omega) \rightarrow L^2(\partial\Omega)$, $f \mapsto u|_{\partial\Omega}$, where $u \in H^1(\Omega)$ solves

$$-\nabla \cdot D \nabla u + u = f, \quad x \in \Omega, \quad (42)$$

$$D \nabla u \cdot \mathbf{n} = 0, \quad x \in \partial\Omega. \quad (43)$$

Unless otherwise stated, the conductivity is assumed to be isotropic, i.e., $D = 1$.

In all the experiments, the exact data was synthetically generated by applying K to a true source f^* , yielding

$$d^\dagger := Kf^*.$$

The data was then corrupted with additive white Gaussian noise to produce the noisy observations

$$d = d^\dagger + \epsilon,$$

where the noise ϵ was scaled to ensure a relative noise level of 1%, i.e.,

$$\frac{\|\epsilon\|}{\|d\|} = 0.01.$$

When solving the discretized problem, we employed the iterative Bregman method presented in [17]:

$$\begin{aligned} \mathbf{x}_{k+1} &= \arg \min_{\mathbf{x}} \left\{ \frac{1}{2} \|\mathbf{Ax} - \mathbf{b}_k\|^2 + \alpha TV_w(\mathbf{x}) + \beta \|\tilde{W}\mathbf{x}\|_1 \right\}, \\ \mathbf{b}_{k+1} &= \mathbf{b}_k + (\mathbf{d} - \mathbf{Ax}_k), \end{aligned} \quad (44)$$

where \mathbf{x} , \mathbf{d} and \mathbf{A} represent discrete counterparts to the source f , the noisy data d and the forward operator K , respectively. The minimization problem in the first step above was solved with the Alternating Direction Method of Multipliers (ADMM) algorithm. We used the standard Morozov discrepancy principle as stopping criterion for the procedure and performed experiments with both $\beta = 0$ and $\beta > 0$.

Remark 7.1. *In the discrete case, we use the $\|\cdot\|_1$ -norm to include sparsity regularization and thus not the measure theoretical approach employed in the infinite dimensional setting considered in Section 6, cf. (32). Nevertheless, results analogous to Proposition 6.1, Lemma 6.3 and Proposition 6.4 can be proven for (44); using very similar arguments to those presented above. Here, \tilde{W} is a diagonal matrix*

$$\begin{bmatrix} \tilde{w}_1 & & \\ & \ddots & \\ & & \tilde{w}_n \end{bmatrix}$$

with entries

$$\tilde{w}_i = \|\mathbf{A}\mathbf{e}_i\|_2, \quad i = 1, 2, \dots, n,$$

or

$$\tilde{w}_i = \|\mathbf{A}_q^\dagger \mathbf{A}\mathbf{e}_i\|_2, \quad i = 1, 2, \dots, n, \quad (45)$$

where $\{\mathbf{e}_i\}$ are the standard Euclidean basis vectors and \mathbf{A}_q^\dagger denotes an approximation of the pseudo inverse of \mathbf{A} , defined in terms of the singular vectors associated with the q largest singular values of \mathbf{A} . In our numerical experiments, we employed the form (45) with $q = 120$.

As mentioned in Remark 5.1, one may define the TV-weights in terms of any L^p -norm. Figure 5 shows the weights computed with $p = 1$ and $p = \infty$, and Figure 6 exemplifies that the choice $p = \infty$ yields somewhat better results than using $p = 1$, especially for small true sources. We therefore below present results computed with $p = \infty$, even though Theorem 5.2 presupposes $p = 1$. The authors regard it as an open problem to formulate conditions similar to (30) and (31) such that Theorem 5.2 also holds for $p = \infty$.

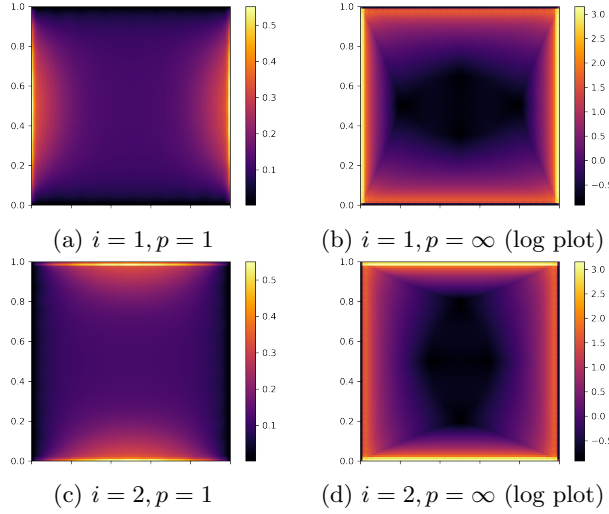


Figure 5: Total variation weights $\|K\partial_{y_i} G(\cdot; y)\|_{L^p(E)}$ for $i = 1, 2$ and different values of p , cf. (27).

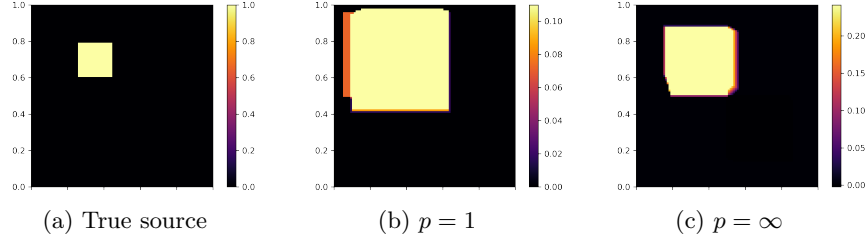


Figure 6: Comparison of the true source and inverse recoveries using weighted TV (TV_w) for different p -norms in the weights $\|K\partial_{y_i}G(\cdot; y)\|_{L^p(E)}$, cf. (27).

Small rectangular source

The first example concerns a small square-shaped (true) source positioned somewhat off the center of the grid, as shown in Figure 7(a). We can observe that the position of the source is recovered using both weighted TV and the hybrid method. However, the size of the true source is clearly overestimated by weighted TV approach, as seen in panel b).

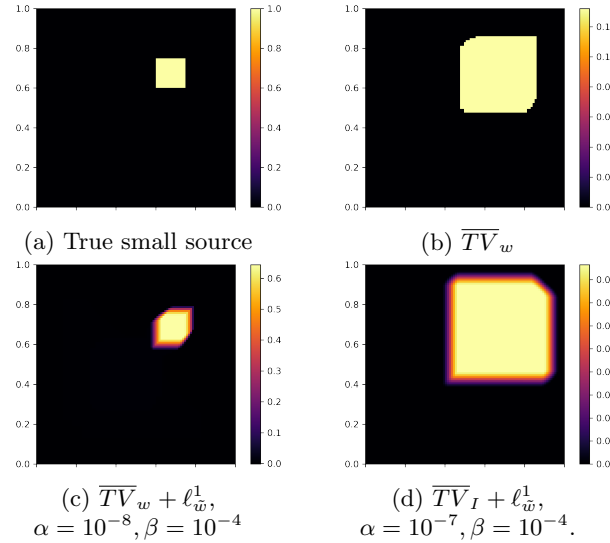


Figure 7: Comparison of the true source and inverse recoveries using weighted TV (TV_w) or unweighted/standard TV (TV_I), as well as hybrid TV and weighted ℓ_w^1 -norm.

Large rectangular source

In contrast to what was observed for the previous setup, the recovery is almost perfect with weighted TV when the true source is a larger square, cf. panels a)

and b) in Figure 8. If we apply the hybrid method with too strong emphasis on the ℓ_w^1 -term, the size of the true source is somewhat underestimated, see panel c).

A rough discussion of why weighted TV handles larger rectangles well, is presented in Section 5 after the proof of Theorem 5.2. BIAS 45 degrees, stairs

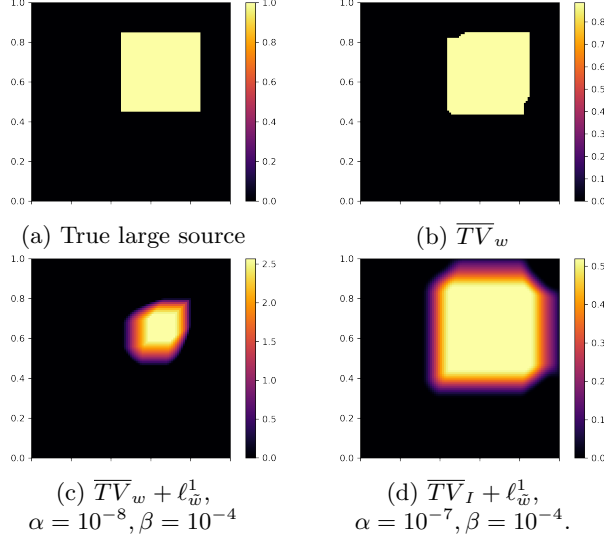


Figure 8: Comparison of the true source and inverse recoveries using weighted TV (TV_w) or unweighted/standard TV (TV_I), as well as hybrid TV and weighted ℓ_w^1 -norm.

Positional influence

The next example illuminates the ability of the methods to locate small true sources in different parts of the domain. When applying weighted TV, we observe that the further into the domain the true source is located, the more its size is overestimated by the inversion procedure, cf. panels (b), (e) and (h) of Figure 9. The use of a hybrid approach can (somewhat) mitigate this problem.

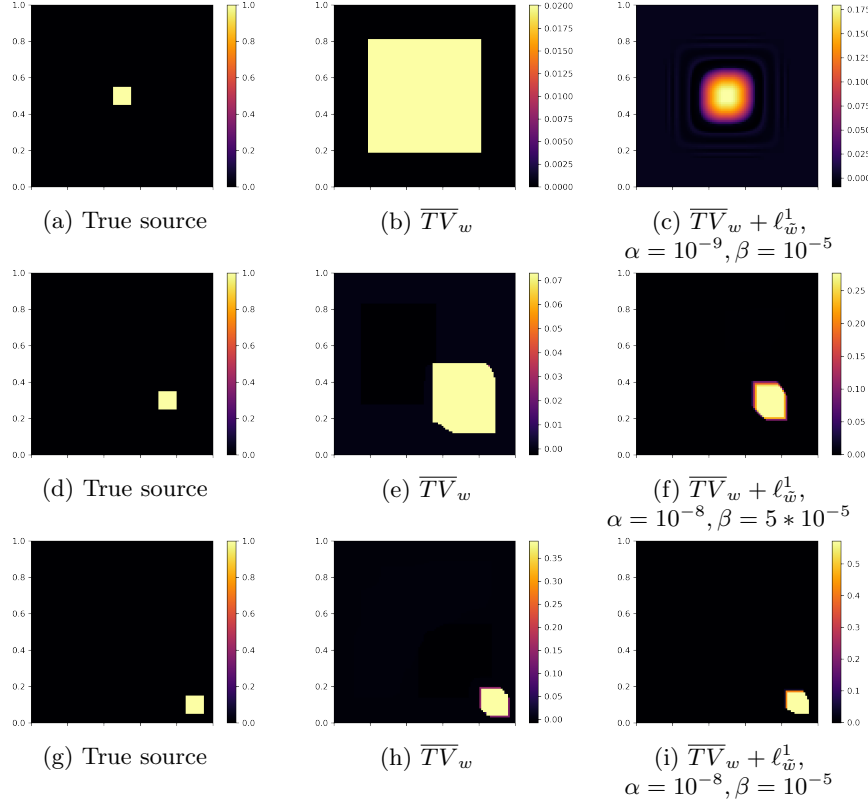


Figure 9: Illustration of how the position of the true source influences the size of the inversely recovered regions.

More advanced shapes

For sources with more complex geometries, as shown in Figure 10, recovering the true source shape becomes increasingly challenging. The weighted TV method tends to produce more block-like reconstructions (middle panels). When the hybrid method is applied (right panels), the reconstruction quality shows a modest but noticeable improvement.

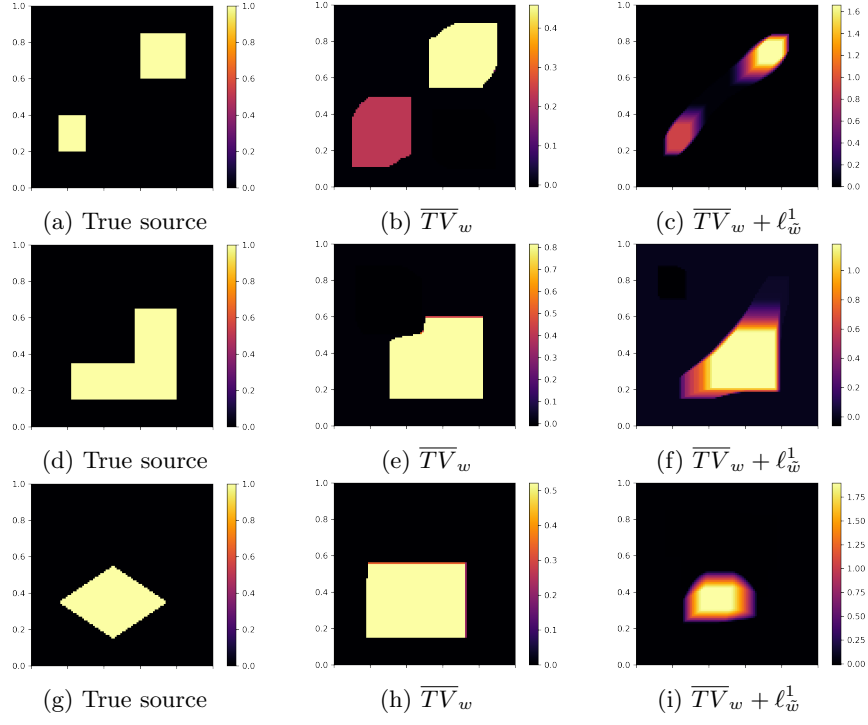


Figure 10: Comparison of true generating source and the recovered source using weighted and unweighted total variation approaches.

Anisotropic conductivity

We will now consider two problems involving anisotropic conductivities, that is, the forward operator now involved the boundary value problem (42)-(43) with D equal to

$$D(x_1, x_2) := D_1(x_1, x_2) = (1 + 9x_1) \begin{bmatrix} 5 & 0 \\ 0 & 1 \end{bmatrix}, \quad (46)$$

and

$$D(x_1, x_2) := D_2(x_1, x_2) = \begin{cases} 10, & x_1 \leq 0.4, x_2 \leq 0.4, \\ 1, & x_1 > 0.4, x_2 > 0.4, \end{cases} \quad (47)$$

respectively.

Figure 11 displays simulations with the conductivity given in (46). The conductivity is strongly increasing in the x_1 -direction, which might explain the somewhat more blurry solution seen in panel h). Nevertheless, the weighted inversion scheme is still able to recover the position of the true sources.

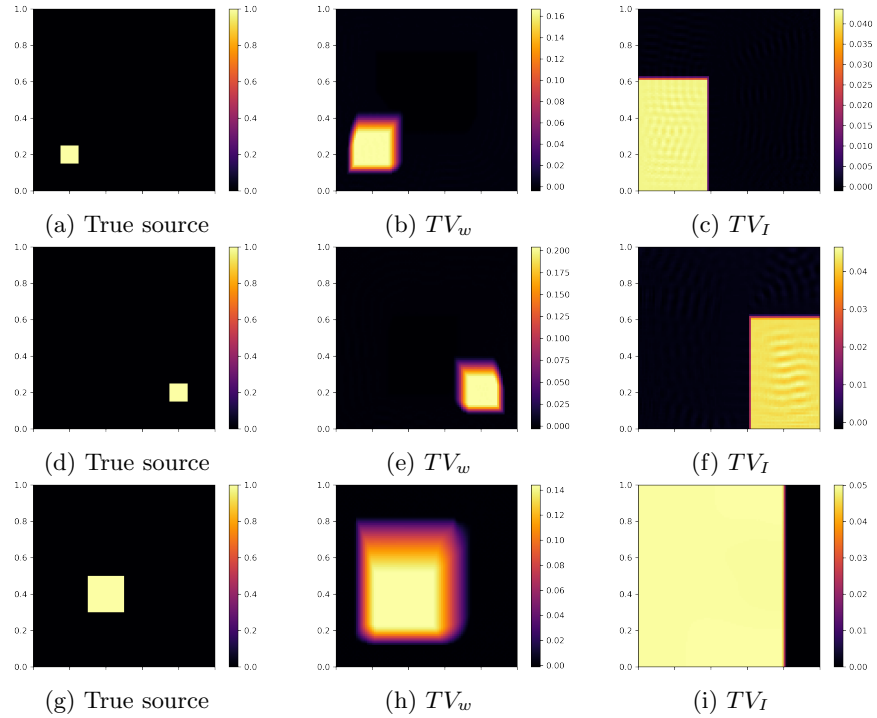


Figure 11: Comparison of true generation source and inverse recovery involving the anisotropic conductivity D_1 , cf. (46).

The weighted TV algorithm for the case with discontinuous conductivity defined in (47) also successfully locates the sources; see Figure 12. Note in particular that the source displayed in panel g) has support at the discontinuity, but this does not seem to affect the ability of the weighted scheme to detect the source.

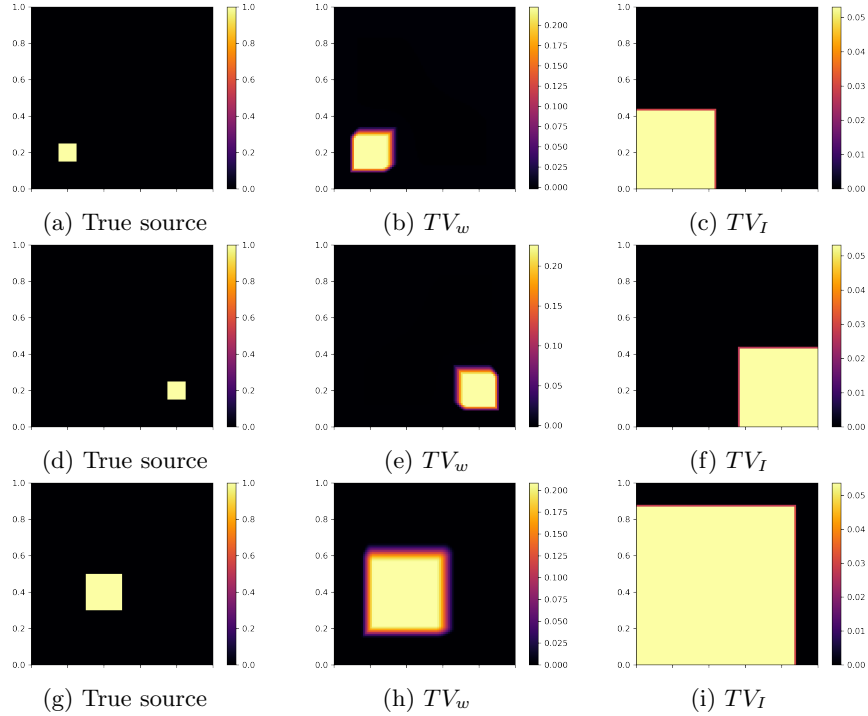


Figure 12: Comparison of true generation source and inverse recovery involving the anisotropic conductivity D_2 , cf. (47).

8 Conclusion

In this paper we have studied the influence of weighting on TV-regularized solutions for inverse problems, which is introduced in order to reduce bias stemming from specific properties of the forward operator. We have seen that appropriate weighting can strongly improve the quality of reconstructions and the position of sources compared to standard TV methods. Compared to previously studied methods, such as weighted ℓ^1 , which prefers zero-dimensional structures, weighted TV enhances codimension-one structures and may introduce some bias on their shape. As a potential alternative, a hybrid method between TV and weighted ℓ^1 can be considered, which seems feasible for inverse source problems with small structures. Naturally, the approach encounters problems for larger shapes.

We finally mention that in order to cure depth bias - as appearing in inverse source problems in EEG/MEG or ECG due to the depth variation of the point-spread (respectively Green's) function - it is crucial to use an extended total variation, which also takes into account the boundary of the domain. The extended version effectively considers the total variation of a function extended by zero outside the domain, thus penalizing structures at the boundary as well.

In general, the choice of the optimal weights in TV and related methods is still a challenging question which might be solved by machine learning techniques for specific applications.

Acknowledgements

MB acknowledges support from DESY (Hamburg, Germany), a member of the Helmholtz Association HGF.

References

- [1] F. Andreu-Vaillo, V. Caselles, and J. M. Mazon. *Parabolic quasilinear equations minimizing linear growth functionals*. Vol. 223. Birkhäuser Verlag, Basel, 2004.
- [2] G. Anzellotti. “Pairings between measures and bounded functions and compensated compactness”. In: *Annali di Matematica pura ed applicata* 135 (1983), pp. 293–318. DOI: [10.1007/BF01781073](https://doi.org/10.1007/BF01781073).
- [3] M. Benning and M. Burger. “Ground states and singular vectors of convex variational regularization methods”. In: *Methods and Applications of Analysis* 20 (2013), pp. 295–334.
- [4] M. Benning and M. Burger. “Modern regularization methods for inverse problems”. In: *Acta Numerica* 27 (2018), pp. 1–111. DOI: [10.1017/S0962492918000059](https://doi.org/10.1017/S0962492918000059).
- [5] K. Bredies and M. Holler. “Higher-order total variation approaches and generalisations”. In: *Inverse Problems* 36 (2020). DOI: [10.1088/1361-6420/ab8f80](https://doi.org/10.1088/1361-6420/ab8f80).
- [6] K. Bredies, J. Iglesias, and G. Mercier. “Boundedness and Unboundedness in Total Variation Regularization”. In: *Applied Mathematics and Optimization* 88 (2023). DOI: [10.1007/s00245-023-10028-y](https://doi.org/10.1007/s00245-023-10028-y).
- [7] K. Bui et al. “A Weighted Difference of Anisotropic and Isotropic Total Variation for Relaxed Mumford–Shah Color and Multiphase Image Segmentation”. In: *SIAM Journal on Imaging Sciences* 14 (2021), pp. 1170–1195. DOI: [10.1137/20M1337041](https://doi.org/10.1137/20M1337041).
- [8] M. Burger. “Nonlinear eigenvalue problems for seminorms and applications”. In: *Proc. Int. Cong. Math.* Vol. 7. 2022, pp. 5234–5255.
- [9] M. Burger, H. Dirks, and J. Müller. “Inverse problems in imaging”. In: *Large Scale Inverse Problems. Computational Methods and Applications in the Earth Sciences* (M. Cullen, M. A. Freitag, S. Kindermann, and R. Scheichl, eds.), *Radon Series on Computational and Applied Mathematics* 13 (2013), pp. 135–180.

- [10] O. L. Elvetun and B. F. Nielsen. “A regularization operator for source identification for elliptic PDEs”. In: *Inverse Problems and Imaging* 15 (2021), pp. 599–618.
- [11] O. L. Elvetun and B. F. Nielsen. “Box constraints and weighted sparsity regularization for identifying sources in elliptic PDEs”. In: *Numerical Functional Analysis and Optimization* (2024), pp. 1–34. DOI: 10.1080/01630563.2024.2405489.
- [12] O. L. Elvetun and B. F. Nielsen. “Identifying the source term in the potential equation with weighted sparsity regularization”. In: *Mathematics of Computation* 93 (2024), pp. 2811–2836.
- [13] O. L. Elvetun and B. F. Nielsen. “Weighted sparsity regularization for source identification for elliptic PDEs”. In: *Journal of Inverse and Ill-posed Problems* (2023). DOI: 10.1515/jiip-2021-0057.
- [14] M. Hintermüller and C. N. Rautenberg. “Optimal selection of the regularization function in a weighted total variation model. Part I: Modelling and theory”. In: *Journal of Mathematical Imaging and Vision* 59 (2017), pp. 498–514.
- [15] M. Hintermüller et al. “Optimal Selection of the Regularization Function in a Weighted Total Variation Model. Part II: Algorithm, Its Analysis and Numerical Tests”. In: *Journal of Mathematical Imaging and Vision* 59 (2017), pp. 515–533. DOI: 10.1007/s10851-017-0736-2.
- [16] M.-M. Li and B.-Z. Li. “A Novel Weighted Total Variation Model for Image Denoising”. In: *IET Image Processing* 15 (2021), pp. 1459–1469. DOI: 10.1049/ipt2.12259.
- [17] S. Osher et al. “An Iterative Regularization Method for Total Variation-Based Image Restoration”. In: *Multiscale Modeling & Simulation* 4 (2005), pp. 460–489. DOI: 10.1137/040605412.
- [18] A. V. Rahiman and S. N. George. “Multi-frame Image Super Resolution Using Spatially Weighted Total Variation Regularisations”. In: *IET Image Processing* 14 (2020), pp. 2187–2194. DOI: 10.1049/iet-ipr.2019.0901.
- [19] X. Sheng, L. Yang, and J. Chang. “Weighted Structure Tensor Total Variation for Image Denoising”. In: *Journal of Electronic Imaging* 33 (2024), p. 013049. DOI: 10.1117/1.JEI.33.1.013049.
- [20] W. P. Ziemer. *Weakly Differentiable Functions*. Springer New York, NY, 1989. DOI: 10.1007/978-1-4612-1015-3.

A Regularized problem, 1D

In this appendix we prove Theorem 4.4. We need two lemmas.

Lemma A.1. *Let $K : L^2(\Omega) \rightarrow L^2(E)$ be linear and let Q be the orthogonal projection defined in (15). Then, for any $f \in L^2(\Omega)$,*

$$K^*Kf = C^*Cf + \frac{(Kf, K1)}{\|K1\|^2} K^*K1,$$

where C is the mapping introduced in (17).

Proof. Note that we can decompose any image Kf by

$$Kf = QKf + \text{proj}_{K1}(Kf) = QKf + \frac{(Kf, K1)}{\|K1\|^2} K1,$$

and consequently

$$K^*Kf = K^*QKf + \frac{(Kf, K1)}{\|K1\|^2} K^*K1.$$

The result follows by observing that $C^*C = (QK)^*QK = K^*Q^*QK = K^*QK$, keeping in mind that Q is an orthogonal projection. \square

Inspired by the characterization of the subdifferential $\partial TV(f)$ presented in, e.g., [6, 1] we will show that

Lemma A.2. *Assume that $\Omega = (0, 1)$ and consider the weighted TV-functional TV_w defined in (7). If $p = -z' \in L^2(\Omega)$ satisfies*

- (i) $|z(x)| \leq w(x) \ \forall x \in (0, 1)$,
- (ii) $\int_0^1 z Df(x) = TV_w(f)$, and
- (iii) $Tz = 0$, where T is the normal trace operator,

then $p \in \partial TV_w(f)$. Furthermore, p has zero mean, i.e., $\int_0^1 p(x)dx = 0$.

Proof. By definition of the subdifferential,

$$p \in \partial TV_w(f) \iff TV_w(g) \geq TV_w(f) + (p, g - f) \quad \forall g \in BV(0, 1).$$

Using the assumptions for z above, we get for any $g \in BV(0, 1)$

$$\begin{aligned} TV_w(f) + (p, g - f) &= - \int_0^1 z'(x)g(x)dx = \int_0^1 z(x)Dg(x) \\ &\leq \int_0^1 |z(x)| |Dg(x)| \leq \int_0^1 w(x) |Dg(x)| \\ &= TV_w(g), \end{aligned}$$

where the integration by parts is justified, e.g., by the generalized Green's theorem [2, Theorem 1.9]. We employed (9) in the last equality.

For the zero mean property, simply choose $g_k \in BV(0, 1)$, $g_k(x) = -k \operatorname{sgn} \left(\int_0^1 z'(x) \right)$ above to get

$$\begin{aligned} TV_w(f) + (p, g_k - f) &= TV_w(f) - \int_0^1 z'(x)g_k(x)dx - TV_w(f) \\ &= k \operatorname{sgn} \left(\int_0^1 z'(x) \right) \int_0^1 z'(x)dx, \end{aligned}$$

which we can make as large as we want, by letting $k \rightarrow \infty$, unless $-z' = p$ has zero mean. Hence, $-z' = p$ must have zero integral because $TV_w(g_k) = 0$ for any constant k . \square

Proof of Theorem 4.4.

Proof. We will prove the theorem by verifying that

$$f_\alpha = \gamma\rho\bar{H}_{x^*} + \eta$$

satisfies the first-order optimality condition

$$K^*K(\rho\bar{H}_{x^*} + \tau) - K^*Kf \in \alpha\partial TV_w(f) \quad (48)$$

associated with (25) for specific choices of γ and η (cf. Theorem 4.4).

Since TV_w is one-homogeneous and does not see constants, it follows that, for $\gamma > 0$,

$$\partial TV_w(f_\alpha) = \partial TV_w(\gamma\rho\bar{H}_{x^*}) = \operatorname{sgn}(\gamma\rho)\partial TV_w(\bar{H}_{x^*}) = \operatorname{sgn}(\rho)\partial TV_w(\bar{H}_{x^*}).$$

Thus, by inserting the expression for f_α into the optimality condition (48), and multiplying both sides by $\operatorname{sgn}(\rho)$, the problem can be reformulated to proving that there exists

$$p \in \partial TV_w(\bar{H}_{x^*})$$

such that

$$K^*K \left((1 - \gamma)|\rho|\bar{H}_{x^*} + \operatorname{sgn}(\rho)(\tau - \eta) \right) = \alpha p. \quad (49)$$

Our strategy for verifying the existence of such an element p in the subdifferential $\partial TV_w(\bar{H}_{x^*})$ will be to initially define z (up to a constant) by

$$-\alpha z' = K^*K \left((1 - \gamma)|\rho|\bar{H}_{x^*} + \operatorname{sgn}(\rho)(\tau - \eta) \right),$$

and thereafter show, for a specific choice of the free constant, that all the assumptions in Lemma (A.2) are satisfied by $p = -z'$, which will yield the desired result.

Since the definition of z depends on the parameters γ and η , we need to determine these quantities. Let us make use of Lemma A.1 to obtain the expression

$$\begin{aligned}
-\alpha z' &= K^* K ((1-\gamma)|\rho| \bar{H}_{x^*} + \operatorname{sgn}(\rho)(\tau - \eta)) \\
&= (1-\gamma)|\rho| C^* C \bar{H}_{x^*} \\
&+ \frac{((1-\gamma)|\rho| K \bar{H}_{x^*} + \operatorname{sgn}(\rho)(\tau - \eta) K 1, K 1)}{\|K 1\|^2} K^* K 1 \\
&= (1-\gamma)|\rho| C^* C \bar{H}_{x^*} \\
&+ \left(\frac{(1-\gamma)|\rho| (K \bar{H}_{x^*}, K 1)}{\|K 1\|^2} + \operatorname{sgn}(\rho)(\tau - \eta) \right) K^* K 1. \quad (50)
\end{aligned}$$

Recall that Lemma A.2 asserts that z' must have zero mean. Since C annihilates constants, the observation that

$$\int_0^1 (C^* C \bar{H}_{x^*})(x) dx = (C^* C \bar{H}_{x^*}, 1) = (C \bar{H}_{x^*}, C 1) = 0,$$

therefore motivates the removal of the last term in (50). Consequently, we must choose

$$\eta = \tau + \frac{(1-\gamma)\rho(K \bar{H}_{x^*}, K 1)}{\|K 1\|^2}.$$

Then (50) simplifies to

$$-\alpha z' = (1-\gamma)|\rho| C^* C \bar{H}_{x^*}, \quad (51)$$

which guarantees that z' has zero mean.

The choice of γ is somewhat more involved, but observe that by multiplying (51) with \bar{H}_{x^*} and integrating, we get

$$\begin{aligned}
\int_0^1 -z'(x) \bar{H}_{x^*}(x) dx &= \frac{(1-\gamma)|\rho|}{\alpha} \int_0^1 C^* C \bar{H}_{x^*}(x) \bar{H}_{x^*}(x) dx \\
&= \frac{(1-\gamma)|\rho|}{\alpha} (C^* C \bar{H}_{x^*}, \bar{H}_{x^*}) \\
&= \frac{(1-\gamma)|\rho|}{\alpha} \|C \bar{H}_{x^*}\|^2 \\
&= (1-\gamma) \frac{|\rho| \|C \bar{H}_{x^*}\|}{\alpha} \|C \bar{H}_{x^*}\| \\
&= \|C \bar{H}_{x^*}\| := TV_w(\bar{H}_{x^*}), \quad (52)
\end{aligned}$$

when

$$\gamma = 1 - \frac{\alpha}{|\rho| \|C \bar{H}_{x^*}\|}. \quad (53)$$

Furthermore, provided that z has zero trace, i.e., $Tz = 0$,

$$\int_0^1 -z'(x) \bar{H}_{x^*}(x) dx = \int_0^1 z(x) D \bar{H}_{x^*}(x). \quad (54)$$

Combining this with (52) would imply that assumption (ii) of Lemma A.2 is satisfied. However, we must make sure that $Tz = 0$. We now address this issue.

Since z' has zero mean, we find that

$$\int_0^1 z'(x)dx = z(1) - z(0) = 0,$$

which implies that $z(0) = z(1)$. This point-wise evaluation is justified because Sobolev's embedding theorem asserts that $z \in C([0, 1])$ provided that $-z' = p \in L^2(0, 1)$. Recall that z is (until now) only defined up to a constant, and we are therefore free to choose this constant such that $z(0) = z(1) = 0$. Thus, the zero trace condition (iii) in Lemma A.2 is satisfied and as a consequence of the discussion above, so is condition (ii).

Finally, it remains to show that $|z(x)| \leq w(x) \forall x \in (0, 1)$, i.e., to verify that requirement (i) in Lemma A.2 holds. Since $D\bar{H}_{x^*}$ is the Dirac measure at x^* , we can write, keeping in mind that z has zero trace,

$$\begin{aligned} |z(x)| &= \left| \int_0^1 z(y) D\bar{H}_x(y) \right| \\ &= \left| - \int_0^1 z'(y) \bar{H}_x(y) dy \right|. \end{aligned}$$

Invoking (51) and the expression (53) for γ now yield that

$$\begin{aligned} |z(x)| &= \left| \frac{1}{\|C\bar{H}_{x^*}\|} \int_0^1 (C^* C \bar{H}_{x^*})(y) \bar{H}_x(y) dy \right| \\ &= \frac{1}{\|C\bar{H}_{x^*}\|} |(C^* C \bar{H}_{x^*}, \bar{H}_x)| \\ &= \frac{1}{\|C\bar{H}_{x^*}\|} |(C \bar{H}_{x^*}, C \bar{H}_x)| \\ &\leq \|C \bar{H}_x\| := w(x), \end{aligned}$$

where we have employed the Cauchy-Schwarz inequality.

Hence, all the requirements needed in Lemma A.2 are satisfied, and we can conclude that $p = -z' \in \partial TV_w(\bar{H}_{x^*})$. Combining this fact with the optimality condition (49) completes the proof. \square